A comparative study of a stochastic and deterministic simulation of strong ground motion applied to the Kozani-Grevena (NW Greece) 1995 sequence

Zafeiria Roumelioti ([1]), **Anastasia Kiratzi** ([1]), **Nikos Theodulidis** ([2]) **and Christos Papaioannou** ([2])

([1]) *Department of Geophysics, Aristotle University of Thessaloniki, Thessaloniki, Greece*

([2]) *Institute of Engineering Seismology and Earthquake Engineering, Thessaloniki, Greece*

Abstract

We present the results of a comparative study of two intrinsically different methodologies, a stochastic one and a deterministic one, performed to simulate strong ground motion in the Kozani area (NW Greece). Source parameters were calculated from empirical relations in order to check their reliability, in combination with the applied methodologies, to simulate future events. Strong ground motion from the Kozani mainshock (13 May, 1995, M_w = 6.5) was synthesized by using both the stochastic method for finite-fault cases and the empirical Green's function method. The latter method was also applied to simulate a M_w = 5.1 aftershock (19 May, 1995). The results of the two simulations computed for the mainshock are quite satisfactory for both methodologies at the frequencies of engineering interest (> ~2 Hz). This strengthens the idea of incorporating proper empirical relations for the estimation of source parameters in *a priori* simulations of strong ground motion from future earthquakes. Nevertheless, the results of the simulation of the smaller earthquake point out the need for further investigation of regional or local, if possible, relations for estimating source parameters at smaller magnitude ranges.

Key words *simulation – ground motion – earthquake – EGF-Kozani*

1. Introduction

During the past decades, much effort has been given to obtaining reliable simulations of strong ground motion generated by finite-faults using methodologies that include theoretical or semi-empirical modelling of the parameters affecting the shape, the duration and frequency content of strong motion records. Even though the performance of these methods has not been comparatively evaluated, so far none appears to be significantly more accurate than to the others. Nevertheless, some of these methods have the advantage of simplicity, as they consider simple models and empirical relations for the representation of source and path processes and so the numerical and analytical difficulties of computing the earth response are avoided.

One of the simplest techniques for predicting strong ground motion from large earthquakes is the Empirical Green's Function (EGF) method. Hartzell (1978) first utilized observed records from small events (*e.g.*, aftershocks and foreshocks) as Green's functions to simulate the mainshock records. Since then, his original idea has been applied, developed, and improved by numerous scientists (*e.g.*, Kanamori, 1979; Had-

Mailing address: Assoc. Prof. Anastasia A. Kiratzi, Department of Geophysics, Aristotle University of Thessaloniki, 540 06 Thessaloniki, Greece; e-mail: kiratzi@geo.auth.gr

ley and Helmberger, 1980; Irikura 1983, 1986; Irikura and Kamae, 1994; Frankel, 1995; Kamae *et al.*, 1998). This particular method has the advantage of collecting the information needed to model the source, path and even site effects from real data.

Another common tool in the simulation of strong ground motion is the stochastic method. This method is based on the stochastic point source model, which stems from the work of Hanks and McGuire (1981) who indicated that the observed high frequency (~1 to 10 Hz) ground motion can be represented by windowed and filtered white noise, with the average spectral content determined by a simple description of the source. The stochastic ground-motion modelling technique, also known as the band limited white-noise method, was first described by Boore (1983). Since then, many researchers have applied the method to simulate ground motion from point sources (*e.g.*, Boore and Atkinson, 1987; Toro and McGuire, 1987; Atkinson and Boore, 1995 among others).

Even though the success of the point-source model has been pointed out repeatedly, it is also well known that it often breaks down, especially near the sources of large earthquakes. Recently, Beresnev and Atkinson (1997) proposed a technique that overcomes the limitation posed by the hypothesis of a point source. Their technique is based on the original idea of Hartzell (1978) to model large events by the summation of smaller ones. In Beresnev and Atkinson (1997) the high-frequency seismic field near the epicentre of a large earthquake is modelled by dividing the fault plane into a certain number of sub-elements and summing their contributions, with appropriate time delays, at the observation point. Each element is treated as a point source with a theoretical ω^{-2} spectrum. A stochastic model is used to calculate the ground-motion contribution from each sub-element, while the propagation effects are modeled empirically.

The investigation of the synthesis of strong ground motion from earthquakes in Greece attracted the attention of many scientists and both stochastic (Papastamatiou *et al.*, 1993; Tolis and Pitilakis, 1993; Margaris and Papazachos, 1994; Margaris and Hatzidimitriou, 1997; Margaris and Boore, 1998) and deterministic approaches (Diagourtas *et al.*, 1993, 1994; Theodulidis and Bard, 1995; Tselentis *et al.*, 1996; Kamae *et al.*, 1998) have been applied.

In this work we present the results of a comparative study of the stochastic method and the EGF method to model the strong ground motion produced by the Kozani-Grevena earthquake of May 13, 1995 (M 6.5). This parallel application was performed in order to evaluate the relative performance of the two methods, in a case where source parameters are calculated from empirical relations. If these empirically estimated source parameters are proven to be adequate to simulate observed ground motions, then empirical regional and local relations for the estimation of source parameters could be very useful in simulations of strong ground motion from future earthquakes.

2. Stochastic approach

The stochastic modelling technique proposed by Beresnev and Atkinson (1997, 1998) is applied in the present study for the simulation of an earthquake of magnitude M_w = 6.5, that occurred in Northwestern Greece (Kozani area) on May 13, 1995. The earthquake caused extensive damage in many villages and some damage in the two large towns of the area, Kozani and Grevena. The mainshock was recorded by an analog accelerograph that had been installed at the building of Prefecture of the city of Kozani by ITSAK (Institute of Engineering Seismology and Earthquake Engineering). This accelerograph was the only one installed within the meizoseismal area by the time of the earthquake occurrence. The obtained record was used for comparison with simulated data.

2.1. *Method*

In the stochastic method, the Fourier amplitude spectrum of a seismic signal is represented as the product of a spectrum, $S(\omega)$, that accounts for the effects of the seismic source and several other filtering functions that represent the effects of the propagation path and the recording site. If the site, where the receiver was installed,

can be characterized as hard rock, the shear-wave acceleration spectrum is given by

$$A(\omega) = 2\omega^2 \cdot S(\omega) \cdot P(\omega) \cdot e^{-\omega R/2Q\beta} \qquad (2.1)$$

where ω is the angular frequency, R is the hypocenral distance, Q is the quality factor introduced to account for the regional inelastic attenuation and β is the shear-wave velocity. The filtering function $P(\omega)$ is used for the commonly observed spectral cut-off above a certain frequency ω_m. According to some scientists, this phenomenon is caused by the processes that take place at the source during the occurrence of an earthquake (Papageorgiou and Aki, 1983; Papageorgiou, 1988). Others believe that it is mainly due to high-frequency attenuation by the near-surface weathered layer (Hanks, 1982; Anderson and Hough, 1984; Beresnev and Atkinson, 1997; Theodulidis and Bard, 1998). In the methodology described, $P(\omega)$ has the form of the fourth-order Butterworth filter

$$P(\omega) = [1 + (\omega/\omega_m)^8]^{-1/2}. \qquad (2.2)$$

The function $S(\omega)$ is calculated as the product of a certain deterministic function (usually the ω-square model), which defines the average shape and amplitude of the spectrum, and a stochastic function (*e.g.*, the Fourier spectrum of windowed Gaussian noise) that accounts for the realistic random character of the simulated ground motion.

The extension of the stochastic model to the finite-fault case demands transformations of the relative theoretical expressions that have been proposed for point sources, in order to account for the finite dimensions of the sources that produce large earthquakes. The fault plane is discretized into a certain number of equal rectangular elements (subfaults) with dimensions $\Delta l \times \Delta w$. Each subfault is then treated as a point source with an ω-square spectrum, which can be fully defined by two parameters: the seismic moment and the corner frequency of the subfault spectrum. The connection between these two parameters and the finite dimensions of the subfaults is established through two coefficients, $\Delta\sigma$ and κ, respectively. In detail, assuming the simple case for which $\Delta l = \Delta w$, the subfault moment (m_0) can be determined from the relation

$$m_0 = \Delta\sigma \cdot \Delta l^3 \qquad (2.3)$$

where $\Delta\sigma$ is a stress parameter, most closely related to the static stress drop (Beresnev and Atkinson, 1998). $\Delta\sigma$ relates the subfault moment to its finite dimensions. On the other hand, κ relates the subfault spectrum corner frequency, f_c, to its finite dimensions, through the relation

$$\kappa = \frac{f_c \cdot \Delta l}{\beta} \qquad (2.4)$$

where β is the shear-wave velocity. The parameter κ actually controls the level of high-frequency radiation in the simulated time-history and is equal to

$$\kappa = \frac{yz}{\pi} \qquad (2.5)$$

where y is the ratio of rupture velocity to shear-wave velocity and z, represents the ratio of the rise time of a small finite source, T, to the rise time of an equivalent point source, $\tau(T/\tau \equiv z)$. The value of z depends on a convention in the definition of the rise time as it is introduced in the exponential functions that describe the ω^{-2} model (Beresnev and Atkinson, 1997). Different conventions lead to different relations between the rise time T and the corner frequency f_c. In the Beresnev and Atkinson (1997) method z is given a value of 1.68 that holds for a «standard» rupture.

2.2. *Application of the stochastic method to the Kozani earthquake*

The synthetic record was calculated for the Kozani station (fig. 1). At the site of the recording station there is an underlying limestone with a thin near-surface layer of colluviums. The site has been characterized as class A site (Margaris and Boore, 1998) according to the shear-wave velocity averaged over the top 30 m ($V_{30} > 750$ m/s). According to this characterization, we used the frequency-dependent amplifi-

cation model of Frankel *et al.* (1996), as proposed by Margaris and Boore (1998). The modelling parameters used for the simulation are summarized in table I.

The length, L, and width, W, of the target fault were calculated from the following empirical relations applicable to the Aegean and surrounding area (Papazachos and Papazachou, 1997):

$$\log L = 0.51M_w - 1.85 \quad (2.6)$$

$$\log W = 0.19M_w - 0.13 \quad (2.7)$$

where M_w is the moment magnitude.

The dimensions estimated for the target fault from the above relations (29×13 km) are close to those determined by Hatzfeld *et al.* (1997) and Papazachos *et al.* (1998) and in good agreement with field observations, as well (Pavlides *et al.*, 1995). The nucleation started at the northeastern termination of the bottom of the fault and propagated radially up to a depth of about 3 km (Papazachos *et al.*, 1998).

The discretization of the target fault was done following a rather empirical rule. According to Beresnev and Atkinson (1998), the corner frequency, f_c, of the subsources must lie below the frequency range of interest, otherwise the sensitivity of the method to subfault size increases. For simulations at frequencies above 0.2 Hz, eqs. (2.4) and (2.5) give a minimum subfault size of $\Delta l \sim 7$ km (assuming $y = 0.8$ and $z = 1.68$ that hold for a «standard» rupture; Beresnev and Atkinson, 1997). So we used this minimum value of Δl and discretized the target fault plane into 3×2 elements, assuming that $\Delta l \approx \Delta w$. The final model used for the target fault is also shown in fig. 1.

The cut-off frequency, f_{max}, of the simulated acceleration spectrum was calculated from an empirical relation proposed by Theodulidis and Bard (1998):

$$\ln(f_{max}) = 3.20 - 0.18M - 0.028\ln R - 0.47S \quad (2.8)$$

where M is magnitude, R is hypocentral distance and S is a variable which takes the value 0 for «rock» sites and 1 for «alluvium». This relation was derived using a set of strong-motion data from 35 shallow earthquakes in Greece.

Table I. Input parameters for the application of the stochastic method of Beresnev and Atkinson (1997).

Parameter	Kozani earthquake (mainshock)
Fault orientation	Strike 240°, Dip 45° (Geological Survey of Japan)
Fault dimensions, $L \times W$ (km)	29×13
Depth to upper edge of the fault (km)	3
Mainshock moment magnitude (M_w)	6.5
Stress parameter (bars)	50
Subfault dimensions, $\Delta l \times \Delta w$ (km)	7.2×6.5
Subfault moment (dyne·cm)	1.05×10^{25}
Number of subfaults	8
Number of subsources summed	6
Subfault corner frequency	0.36
Crustal shear-wave velocity (km/s)	3.4
Crustal density (g/cm^3)	2.72
Distance-dependent duration term (s)	Duration equal to source rise time
Geometric spreading	1/R
$Q(f)$	$103.5 \times f^{0.89}$
Windowing function	Saragoni-Hart
f_{max} (Hz)	7

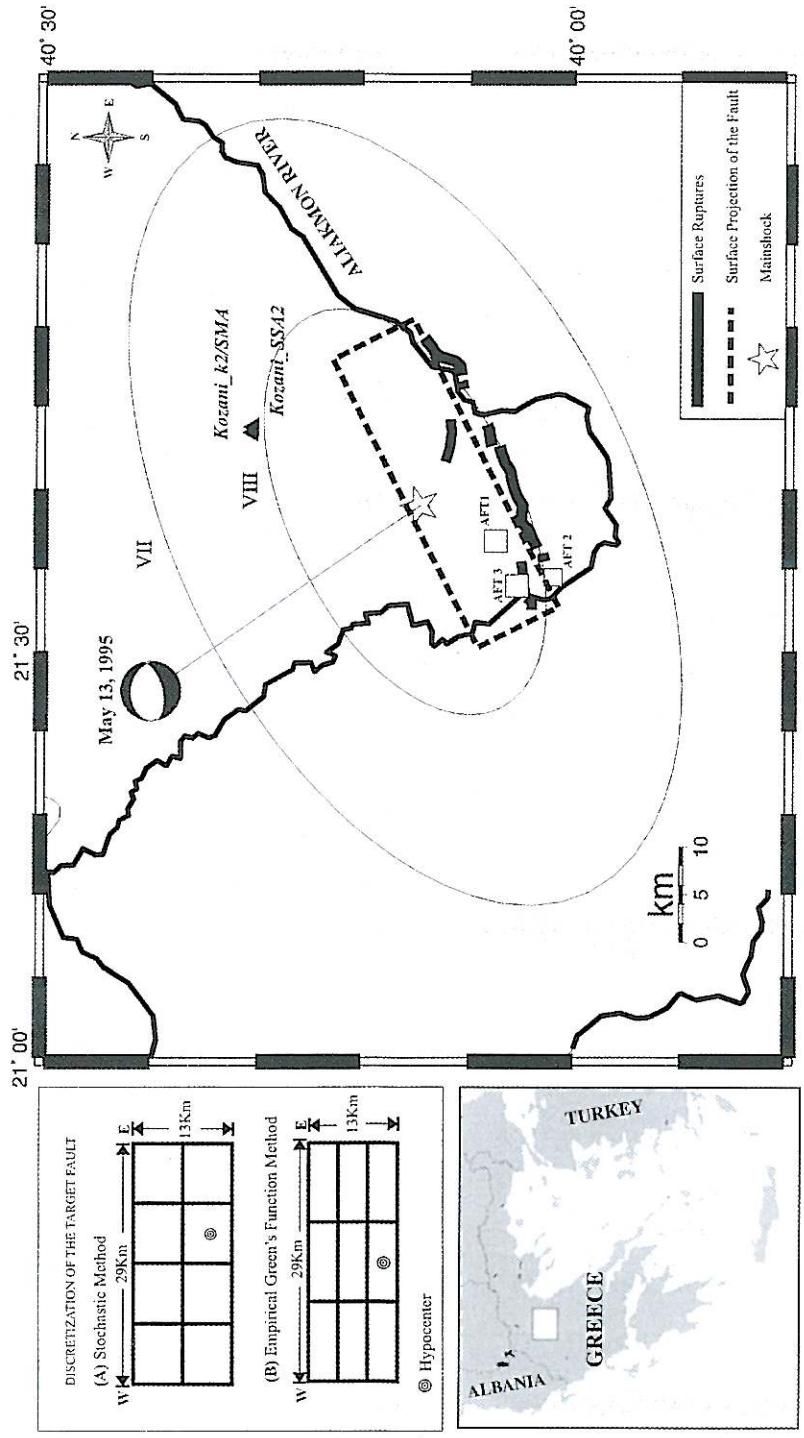

Fig. 1. Regional map showing epicentre (star) and isoseismals (Papazachos *et al.*, 1997) for the Kozani mainshock and epicentres of the other three earthquakes (squares) used in the simulations. The dashed line represents the surface projection of the mainshock fault and the thick continuous line represents surface ruptures observed in the field (Pavlides *et al.*, 1995). The mainshock fault discretizations while applying the stochastic method (A) and the EGF method (B) are also shown.

Even though this value of f_{max} could have been derived with more accuracy from the observed spectrum, we preferred to use a regional empirical relation in order to restrain the *a posteriori* character of the simulation. However, we checked f_{max} of the observed spectra as well, and we found approximately the same value ($f_{max} = 6$).

The same reasoning applies to the calculation of the stress parameter, $\Delta\sigma$, which was assumed equal to 50 bars, a mean value proposed by Kanamori (1979), instead of 63 bars that were calculated for the Kozani mainshock (Margaris and Boore, 1998).

For the geometric attenuation we apply the $1/R$ model and for the inelastic attenuation we use the model of Baskoutas *et al.* (1998), calculated from the coda waves of 80 aftershocks of the Kozani sequence. The duration is kept to be equal to the source rise time at all distances.

2.3. *Results*

Figure 2 compares the simulated *S*-wave part of a random horizontal component to the observed horizontal accelerograms (K2/SMA records). The duration and shape of the observed ground motion are closely predicted. The prediction error of peak acceleration is ~ 7% (the error is calculated as the difference between simulated and observed peak acceleration, divided by observed peak acceleration).

In fig. 3, the simulated Fourier amplitude spectrum is compared with both observed spectra (longitudinal and transverse components) after the application of a moving average smoothing window (every 0.5 Hz with an overlapping step of 0.25 Hz). The matching is quite satisfactory although for frequencies less than 2 Hz and for the recorded *T*-component a small discrepancy is observed.

3. Empirical Green's function approach

We applied the methodology of Irikura (1983, 1986) in order to simulate the observed strong ground motion from the Kozani mainshock (M_w 6.5) using one of its aftershocks (M_w 5.1). We chose the Kozani mainshock because its acceleration records had already been simulated by means of the stochastic method and therefore we could compare the relative performance of the two methodologies applied in the particular area. We also attempted to simulate an aftershock ($M_w = 5.1$) in order to check the effectiveness of the method in synthesizing strong motion from moderate earthquakes. These events have often been proved to be catastrophic in the area of Greece (*e.g.*, on July 14, 1993, an earthquake with $M_L = 5.1$ caused a lot of damage in the city of Patras). Thus we modelled the M_w 5.1 event using one of its very small aftershocks (M_w 4.0). Furthermore, this particular aftershock was recorded by a digital accelerograph and we also had many digital records, which could be used as empirical Green's functions. Since we had the advantage of choosing the best-input data, this simulation was performed as a validation test of the methodology combined with empirical relations for the estimation of source parameters.

3.1. *Method*

Irikura (1983) combined the EGF technique with similarity laws of earthquakes using the dislocation model of Haskell (1964). Under the similarity assumption, when two events with different magnitude occur within the same seismic source, the following similarity relations can be derived:

$$\frac{L}{L_e} = \frac{W}{W_e} = \frac{D}{D_e} = \frac{\tau}{\tau_e} = \left(\frac{M_0}{M_{0e}}\right)^{\frac{1}{3}} = N \qquad (3.1)$$

where L and W are length and width, respectively, of the rectangular seismic source, D is the final offset of the dislocation, τ is the rise time and M_0 is the seismic moment. The parameters without subscript are for the larger event and those with subscript, e, are for the small event. N is the scaling parameter (equal to the closest integer), necessary for the discretization of the target fault.

Irikura and Kamae (1994) revised relation (3.1) to allow for the probable difference in

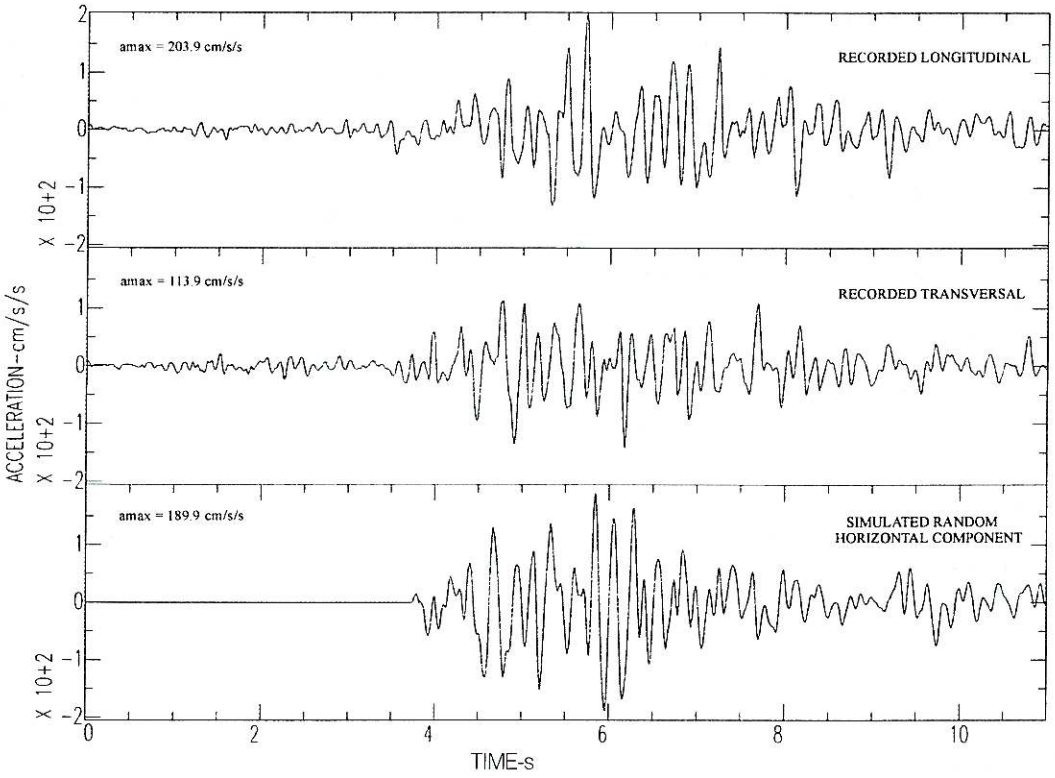

Fig. 2. Comparison of horizontal acceleration time histories recorded at the Kozani station during the 13 May 1995 Kozani earthquake, with the *S*-wave part of a random horizontal component simulated with the Beresnev and Atkinson (1997) method. Peak accelerations in cm/s^2 are shown for each accelerogram.

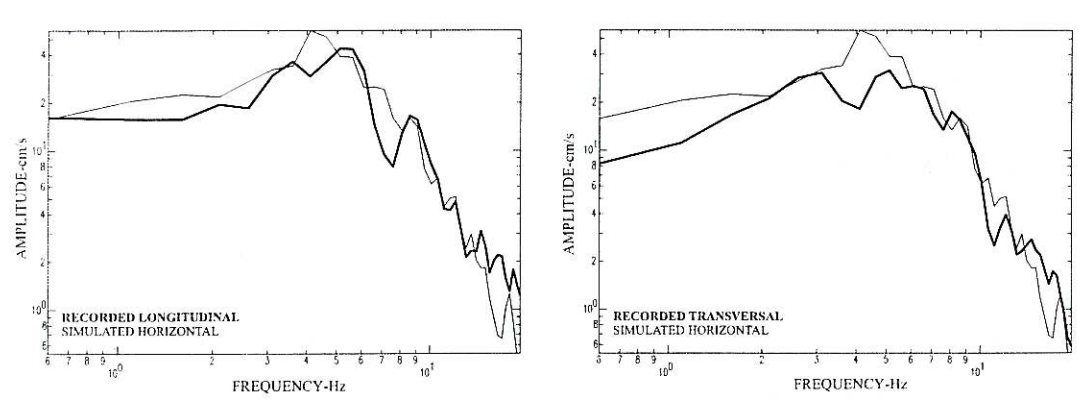

Fig. 3. Observed Fourier amplitude spectra (thick line) of the two horizontal components recorded at the Kozani station are compared with the simulated spectrum (thin line) obtained by the Beresnev and Atkinson (1997) method.

stress drop between the large and the small event. The revised relations are

$$\frac{L}{L_e} = \frac{W}{W_e} = \frac{D}{CD_e} = \frac{\tau}{\tau_e} = \left(\frac{M_0}{CM_{0e}} \right)^{\frac{1}{3}} = N \quad (3.2)$$

where C is the ratio of the stress drop of the large event to the stress drop of the small event. Kamae *et al.* (1998) emphasized the importance of the parameter C in the correct estimation of the simulated spectrum level.

The other similarity law used in the methodology described is the ω-square spectral scaling of source spectra, which can be briefly described by the equations

$$\frac{U_0}{U_{0e}} = \frac{M_0}{M_{0e}} = CN^3 \quad (3.3)$$

and

$$\frac{A_0}{A_{0e}} = CN \quad (3.4)$$

where U_0 and A_0 correspond to the flat level of the displacement spectrum and the flat level of the acceleration spectrum, respectively. These relations can be used to calculate the two parameters, C and N, only in cases of *a posteriori* simulations as they imply that the spectrum of the target event must be known.

The seismogram $A(t)$ of the target event is calculated from the relation

$$A(t) = \sum_{i=1}^{N^2} \frac{r}{r_i} F(t - t_i) * Ca(t)$$

where

$$F(t) = \delta(t) + \frac{1}{n'} \sum_{j=1}^{(N-1)n'} \delta \left[t - \frac{(j-1)T}{(N-1)n'} \right] \quad (3.5)$$

and

$$t_i = \frac{r_i}{V_c} + \frac{\xi_i}{V_r} + e_i \cdot$$

In the above relations $a(t)$ is the seismogram of the small event, r is the hypocentral distance of the small event, r_i is the distance of the observation point to the centre of the subfault i, ξ_i is the distance of the rupture initiation point to the centre of the ith subfault, V_r is the rupture velocity, V_c is the velocity of the seismic waves studied, T is the rise time of the large event and n' an integer to eliminate spurious periodicity (Irikura, 1983). The symbol (*) denotes convolution. The function $F(t)$ is introduced to account for a difference in the slip time function of the large event and that of the small event. The first term of the right hand part of eq. (3.5) represents a delta function, $\delta(t)$, and the second term represents a square pulse of duration T. e_i is a random number between $-cw/V_r$ and $+cw/V_r$ $(0 < c < 1)$ used to give a random character to the rupture propagation process (Kamae *et al.*, 1998).

3.2. *Application of the method*

The values of the source parameters used as input data (seismic moment, M_0, fault length, L, fault width, W, stress drop, $\Delta\sigma$, rise time, τ) were estimated from empirical scaling relations, instead of the spectral scaling relations (3.3) and (3.4). We arbitrarily extrapolated these empirical relations to smaller magnitude ranges, in some cases. However, we checked the relevant values from eqs. (3.3) and (3.4) and we found comparable results.

Seismic moment, M_0, was determined from magnitude, M_w, using an empirical relation proposed for Greece and the surrounding area by Papazachos and Papazachou (1997)

$$\log M_0 = 1.5 M_w + 15.99. \quad (3.6)$$

Assuming that the moment magnitudes of the target event and the small event are known, the fault length, L, and fault width, W, were estimated from the eqs. (2.6) and (2.7), respectively. Fault area, S, was estimated from the relation (Papazachos and Papazachou, 1997)

$$\log S_0 = 0.70 M_w - 1.98. \quad (3.7)$$

The static stress drop, $\Delta\sigma$, was estimated from the scalar seismic moment and the fault dimensions using the relation proposed by Keilis-Borok (1959)

$$\Delta\sigma = \frac{7M_0}{16r^3} \quad (3.8)$$

where r is the radius of the circular fault considered in Brune's model (1970, 1971).

Finally, the rise time, τ, was estimated from the empirical relation (Geller, 1976)

$$\tau = \frac{16 S^{1/2}}{(7\pi^{3/2}\beta)} \qquad (3.9)$$

where $S = (L \times W)$ is the fault area and β is the shear-wave velocity.

After having estimated the source parameters of the two events, the target fault was discretized into $N \times N$ subelements. N is the closest integer to the value calculated from the equation

$$N = \left(\frac{M_0}{C \cdot M_{0e}} \right)^{\frac{1}{3}} \qquad (3.10)$$

where

$$C = \frac{\Delta\sigma}{\Delta\sigma_e}. \qquad (3.11)$$

In eqs. (3.10) and (3.11), M_0 and M_{0e} are the seismic moment of the large event and the seismic moment of the small event, respectively, and C is the ratio of the stress drop between both events. The parameters used for the two simulations are listed in table II.

3.3. *Simulation of the M_w 5.1 earthquake with the EGF method*

We simulated a moderate size event, M_w 5.1, using an event of M_w 4.0 as empirical Green's function. The epicentres of the two earthquakes are shown in fig. 1 (AFT3 and AFT2, respectively). Event AFT2 was selected from the data set of similar magnitude aftershocks because its epicentre was very close to that of the target event. The parameters N and C (eqs. (3.10) and (3.11) used for the simulation were estimated to be 2 and 3, respectively. Fault strike, dip, and rake for each one of the two events were derived from the corresponding representative focal mechanisms, calculated by Papazachos *et al.* (1998). We used S-wave velocity of 3.4 km/s (Calganile *et al.*, 1982; Papazachos and Nolet, 1997) and rupture velocity of 2.5 km/s ($V_r = 0.72\beta$). We carried out four simulations of the expected acceleration time history at the Kozani station by changing the nucleation point and assuming that the rupture spread circularly from that point. The effect of the starting point proved to be not so important to the simulation, probably because the fault area of the target event is small relative to the epicentral distance of the simulation site.

Table II. Input parameters for the two applications of the EGF technique.

Parameter	Simulation of the M_w 5.1 event		Simulation of the mainshock	
	Target Event/fault	Small Event/fault	Target Event/fault	Small Event/fault
M_w	5.1	4.0	6.5	5.1
M_0 (dyne · cm)	4.4×10^{23}	9.8×10^{21}	5.5×10^{25}	4.4×10^{23}
Epicentre	40.054°N	40.028°N	40.146°N	40.083°N
Coordinates	21.580°E	21.591°E	21.679°E	21.591°E
Strike (°)	247	265	240	247
Dip (°)	52	46	45	49
Rake (°)	−92	−80	−101	−100
Hypocentral depth (km)	7	1	13	9
Fault length (km)	6	3	29	6
Fault width (km)	6	3	13	6
Rise time (s)	0.75	0.375	2.33	0.75

Figure 4 (upper part) shows the observed records of the M_w 4.0 event, which acts as the Green's function, the observed records (middle part) of the target event of M_w 5.1 and its simulated records (lower part). All accelerograms were recorded at the Kozani station (Kozani_SSA2 in fig. 1). The synthetic waveforms, like the original data, were band-pass filtered between 0.3 and 40.0 Hz.

From fig. 4 we can see that the simulated records reasonably well agree with the observed ones, both as to their amplitude level and their duration. The envelope function of the observed ground motion is also closely predicted. The observed and simulated Fourier amplitude spectra are also compared in fig. 5a. A moving average smoothing was applied to the simulated spectra, as previously described. The agreement between observed and simulated spectra is satisfactory at frequencies higher than ~3 Hz, but at lower frequencies observed amplitude spectra are larger than simulated ones. This is probably due to the lack of low-frequency energy (< 3 Hz) of the small earthquake compared to the relative energy of the target earthquake (fig. 5b).

3.4. *Simulation of the mainshock with the EGF method*

The same methodology was also applied for the simulation of the Kozani mainshock (M_w 6.5). The mainshock was recorded by an analog accelerograph at the Prefecture building of Kozani (Kozani_k2/SMA in fig. 1). Unfortunately no records of large aftershocks with epicentres close to the epicentre of the target event were available, in order to use them as empirical Green's functions. The closest aftershocks with $M_w > 5$ occurred at a distance of about 10 km southwest of the mainshock and were recorded by the same analog accelerograph as the mainshock. Besides the differences in the propagation path we also had to take into account the quality of the analog recordings concerning the early arrivals. We finally used as empirical Green's function the acceleration record of the first large aftershock of the sequence (M_w 5.1) that occurred on May 15, 1995 (AFT1 in fig. 1). The modelling parameters for this simulation are also shown in table II.

The parameters N and C (eqs. (3.10) and (3.11)) were found to be equal to 3 and 4.1, respectively. The values of the S-wave velocity and the rupture velocity were maintained as in the previous simulation. The orientation of the target fault was taken from the focal mechanism estimated by Hatzfeld *et al.* (1997), while for the small earthquake we adopted an orientation proposed by Papazachos *et al.* (1998). In this latter work, after an examination of the focal mechanisms of a large number of shocks that followed the Kozani earthquake, seven clusters of aftershocks were defined and a representative focal mechanism was determined for each of these clusters. In the present simulation, we used the representative focal mechanism that corresponds to the cluster nearest to the epicentre of the EGF event. Finally, we assumed that during the mainshock the rupture started from the deepest central part of the fault (see fig. 1) and spread circularly upwards.

Figure 6 shows the comparison between the synthetic waveforms and the observed ones. We failed to predict the initial P-wave part of the record, mainly due to the quality of the analog input data. The level of the simulation accuracy is quite satisfactory for the rest of the waveform, despite the difference in the propagation path between the small earthquake and the target event. Both, the maximum amplitude as well as the duration of the S-wave part are very closely predicted.

Figure 7a compares the observed spectra to the smoothed simulated spectra. The matching is satisfactory at the frequency band of 0.3 to about 6 Hz and much better at low frequencies than at the previous simulations. However, a larger difference can be noticed at higher frequencies (> 6 Hz), in contradiction again with the previous simulation. A similar difference in the high-frequency energy content between the EGF and the target event emerges from the comparison of their amplitude spectra (fig. 7b). Since the recording site is common for both the small event and the target event, the difference in the recorded high frequencies can be attributed to either source effects or path effects. So the misfit in high frequencies between the observed

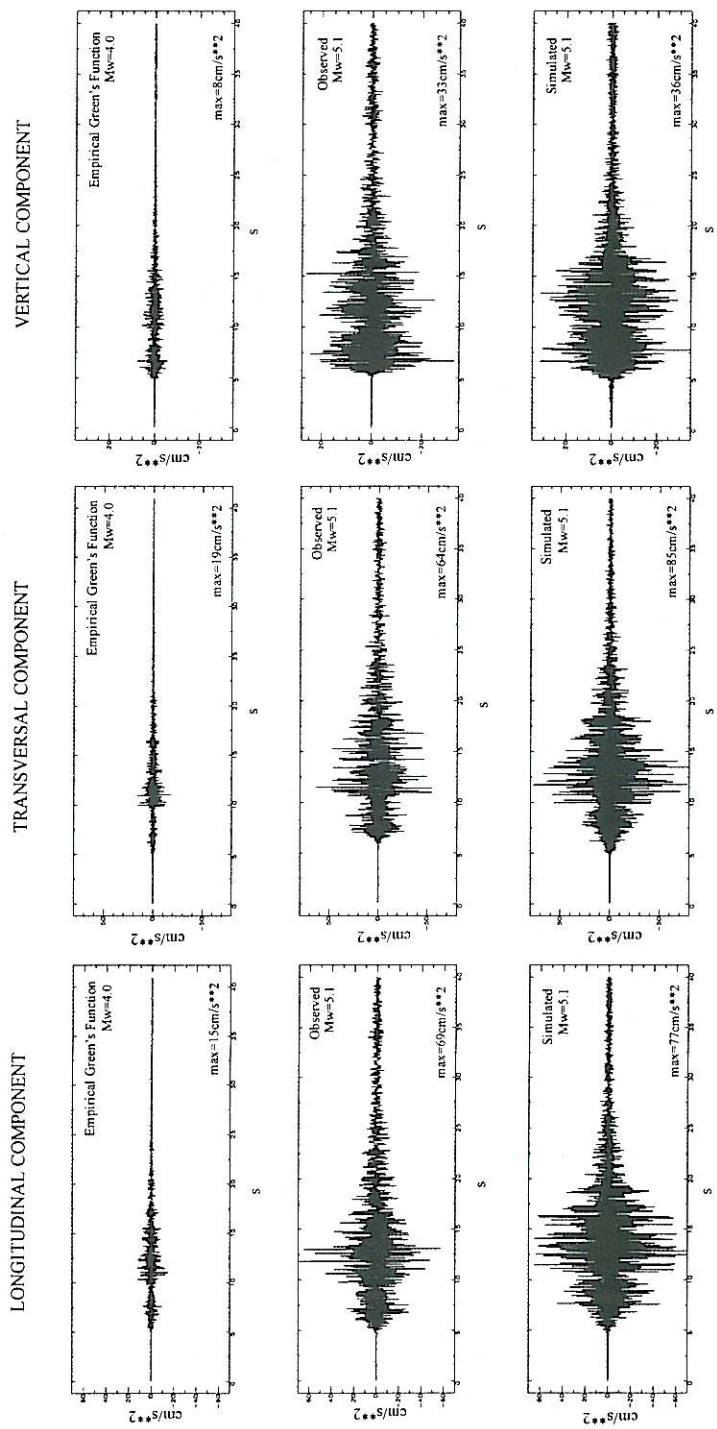

Fig. 4. Observed accelerograms of the small event (M_w 4.0) and the target event (M_w 5.1) together with the simulated accelerograms (EGF method) for the target event, at the Kozani station. Peak accelerations in cm/s^2 are shown for each record.

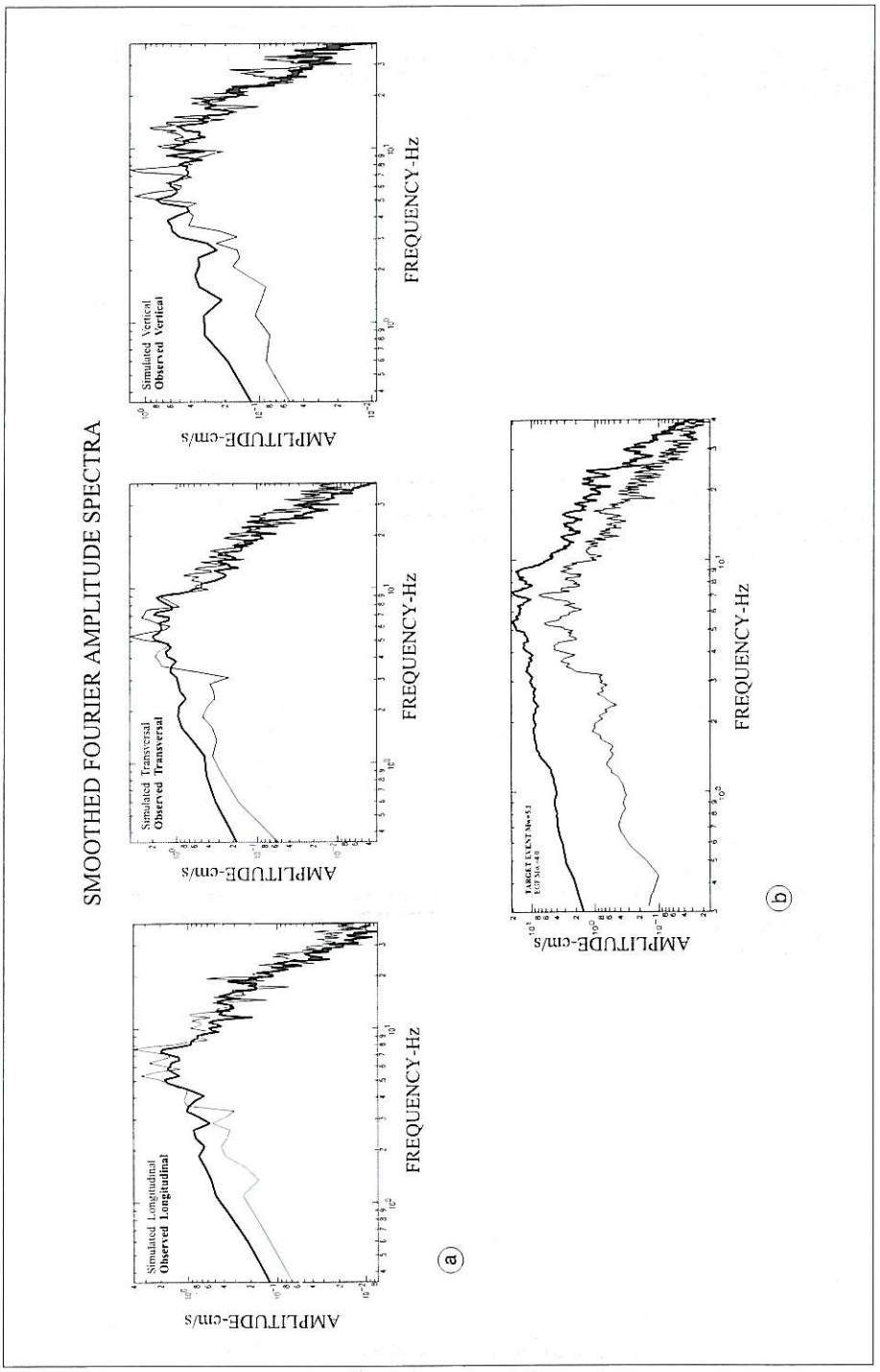

Fig. 5a,b. a) Comparison of the Fourier amplitude spectra at the Kozani station. Thick and thin lines show the observed and simulated spectra for the M_w = 5.1 event, respectively, for each one of the three components; b) Comparison of the smoothed Fourier amplitude spectrum (transversal component) of the target event (thick line) with the relative spectrum of the EGF (thin line).

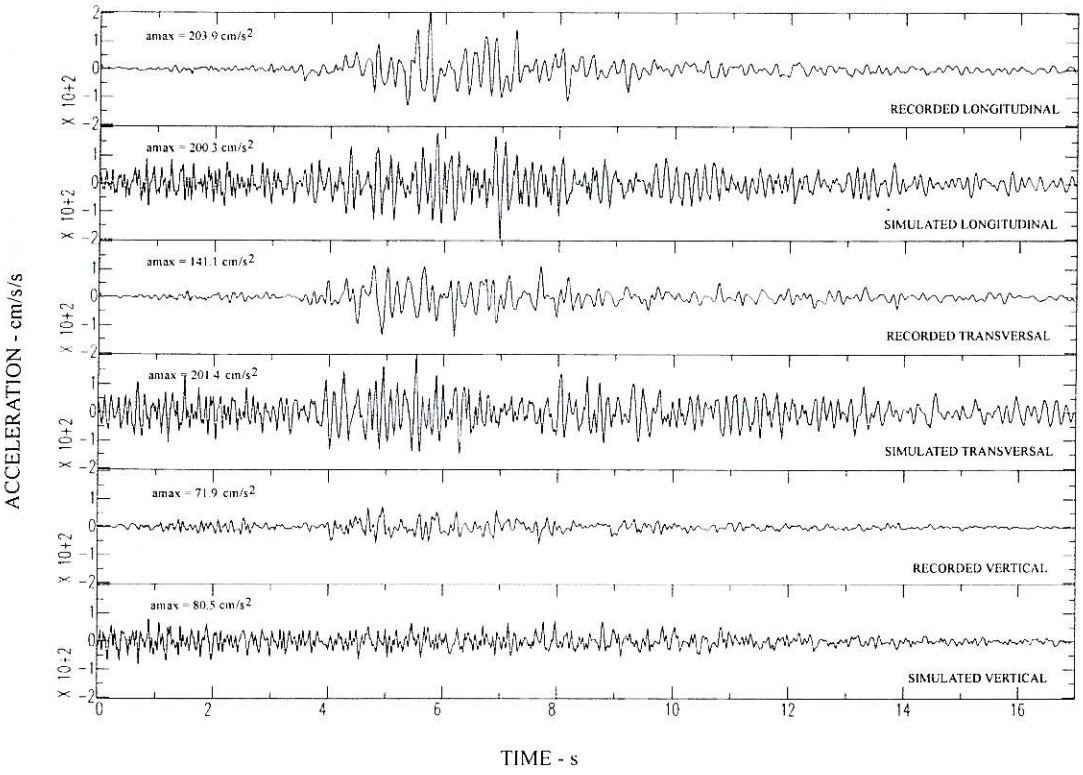

Fig. 6. Comparison of the acceleration time histories, recorded at the Kozani station during the 13 May 1995 mainshock, with the simulated accelerograms by the methodology of Irikura (1993). Peak accelerations in cm/s^2 are also shown for comparison.

spectrum and the simulated spectrum could be due either to inaccurate estimation of source parameters from the empirical relations or to the difference in propagation path between the EGF and the mainshock.

4. Conclusions - discussion

A parallel application of a stochastic and a deterministic method concerning the simulation of strong ground motion was performed to data obtained from the Kozani-Grevena (M_w 6.5) 1995 earthquake sequence in Northwestern Greece.

The stochastic method for finite-fault cases, as proposed by Beresnev and Atkinson (1997), was applied for the simulation of the Kozani mainshock. The *S*-wave part of the observed record was successfully synthesized for frequencies > 2 Hz which is a quite satisfactory result taking into account the use of empirical relations to estimate the fault dimensions, the cut-off frequency (f_{max}) of the target spectrum and the random slip distribution model assumed. The only *a posteriori* knowledge in this simulation was the rupture geometry. Even though such information is not known for a future earthquake, several realistic scenarios can be assumed in order to apply this methodology to estimating average response spectra.

The empirical Green's function (EGF) method was applied, at first, to simulate a moderate event of magnitude M_w 5.1. The simulation was successful for frequencies > 3 Hz, even though

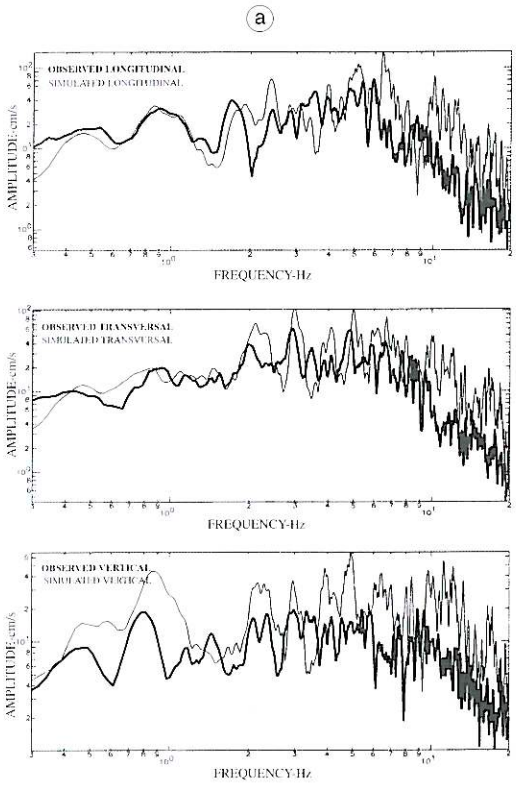

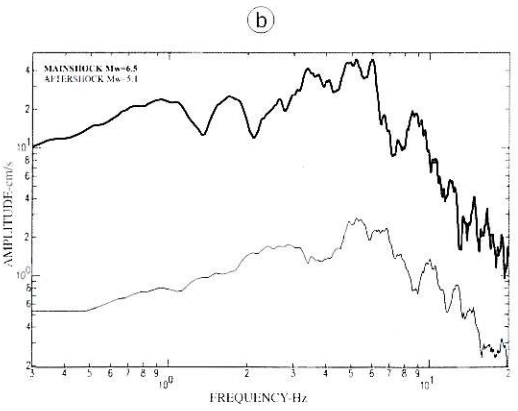

Fig. 7a,b. a) Comparison of the observed Fourier amplitude spectra (thick line) at the Kozani station during the 1995 Kozani mainshock, with the respective simulated spectra (thin line) by the methodology of Irikura (1993). b) Comparison of the smoothed Fourier amplitude spectrum (longitudinal component) of the mainshock (thick line) with the relevant spectrum of the EGF (thin line).

discrepancies were observed for lower frequencies. A second application was made to simulate the ground motion produced by the mainshock (M_w 6.5), giving satisfactory results in the frequency band 0.3 to about 6 Hz, thus, in this case we managed to obtain a good match for lower frequencies as well.

The two methodologies applied gave credible ground motion synthetics, especially for the frequency band relevant to engineering applications. The empirical Green's function method resulted in a better fit between observed and synthetic accelerograms than the stochastic method, mainly due to the information contained in the small earthquake record that was used to describe the Green's function. Even though the maximum amplitude of the synthetics, in the EGF method, is strongly dependent on the value of the parameter C (eq. (3.11)), simulations of the duration of the target earthquake seem to be very stable. The stochastic method, on the other hand, incorporates the available seismological and geological information for a region and does not need specific data in order to be applied.

A basic disadvantage of the EGF method, usually mentioned, in many cases, is the lack of small earthquake recordings. In Greece, the strong motion database is relatively new. However, it is growing rapidly because of the high seismicity of the area and the increase in available instruments. Small earthquake recordings can be readily obtained within relatively short time intervals in most areas of interest and the methodology can be easily applied, at least for the simulation of moderate magnitude earthquakes, that proved to be of great importance in Greece.

Earthquakes in Greece with magnitude greater than 7.0 usually occur at sea and even though they represent a permanent threat for many coastal areas, they are not as catastrophic as earth-

quakes occurring on the mainland. According to the recent seismological history of the area for the past two decades, six earthquakes of magnitude less than 7.0 caused extensive damage and even human losses occurred in many populated areas (Magnesia, 1980, M = 6.6; Alkionides, 1981, M = 6.7; Kalamata, 1986, M = 6.0; Kozani, 1995, M = 6.5; Aigio, 1995, M = 6.4; Konitsa, 1996, M = 5.8; Athens, 1999, M = 5.9). These examples warrant the study of strong ground motion from future events of similar magnitudes. On the other hand, these magnitude ranges are not alarming for non-linear phenomena, at least at far and intermediate field. So, the assumption of linear response of the ground can usually hold.

The main problem is focusing in the near field, where the investigation of strong ground motion has significantly lagged. Most of the methodologies proposed for the simulation of strong ground motion, including the two methodologies applied in the present paper, take into account only far-field terms. In Greece, near field strong ground motion studies are imperative because the mainland is densely cut by active faults, some of which border on large cities or important lifelines. So, even though the potential of the two methods is good, future investigations must focus on the incorporation of near-field terms when predicting strong ground motion.

Acknowledgements

Thanks are due to Prof. I. Beresnev and Prof. K. Irikura for kindly offering the simulation codes and valuable advice. This work was partially funded by the Science for Peace Project (SfP 972342 Seis-Albania) and by Egnatia Odos S.A. (Contract No.: 0000/406/GD/A01/10-11-1999).

REFERENCES

ANDERSON, J. and S. HOUGH (1984): A model for the shape of the Fourier amplitude spectrum of acceleration at high frequencies, *Bull. Seismol. Soc. Am.*, **74**, 1969-1993.

ATKINSON, G.M. and D.M. BOORE (1995): Ground-motion relations for Eastern North America, *Bull. Seismol. Soc. Am.*, **85**, 17-30.

BASKOUTAS, I.G., G.N. STAVRAKAKIS and I.S. KALOGERAS (1998): Q factor estimation from the aftershock sequence of the 13th May 1995 Kozani earthquake, *J. Geodyn.*, **26** (2-4), 367-374.

BERESNEV, I.A. and G.M. ATKINSON (1997): Modelling finite-fault radiation from the ω^n Spectrum, *Bull. Seismol. Soc. Am.*, **87**, 67-84.

BERESNEV, I.A. and G.M. ATKINSON (1998): FINSIM – a FORTRAN program for simulating stochastic acceleration time histories from finite faults, *Seismol. Res. Lett.*, **69**, 27-32.

BOORE, D.M. (1983): Stochastic simulation of high-frequency ground motions based on seismological models of the radiated spectra, *Bull. Seismol. Soc. Am.*, **73**, 1865-1894.

BOORE, D.M. and G.M. ATKINSON (1987): Stochastic prediction of ground motion and spectral response parameters at hard-rock sites in Eastern North America, *Bull. Seismol. Soc. Am.*, **77**, 440-467.

BRUNE, J.N. (1970): Tectonic stress and the spectra of seismic shear waves from earthquakes, *J. Geophys. Res.*, **75**, 4997-5009.

BRUNE, J.N. (1971): Correction, *J. Geophys. Res.*, **76**, 5002.

CALGANILE, G., F. D'INGEO, P. FARRUGIA and G.F. PANZA (1982): The lithosphere in the Central-Eastern Mediterranean area, *Pageoph*, **120**, 389-406.

DIAGOURTAS, D., K.C. MAKROPOULOS, J.-C. GARIEL, N. WAJEMAN, D. HATZFELD and P.-Y. BARD (1993): Simulation of strong ground motion using empirical Green's function method, Preliminary result from an experiment in Greece, in *Proceedings 2nd Hellenic Geophysics Congress*, May 5-7, 1993, Florina, vol. I, 222-235.

DIAGOURTAS, D., K.C. MAKROPOULOS, J.-C. GARIEL, N. WAJEMAN, D. HATZFELD and P.-Y. BARD (1994): Simulation of strong ground motion of the 14 July 1993 Patras earthquake and its contribution to the assessment of seismic hazard, Patras region, W. Greece, in *Proceedings XXIV General Assembly ESC*, September 19-24, Athens, vol. 3, 1446-1454.

FRANKEL, A. (1995): Simulating strong motions of large earthquakes using recordings of small earthquakes: the Loma Prieta mainshock as a test case, *Bull. Seismol. Soc. Am.*, **85**, 1144-1160.

FRANKEL, A., C. MUELLER, T. BARNHARD, D. PERKINS, E.Y. LEYENDECKER, N. DICKMAN, S. HANSON and M. HOPPER (1996): National seismic hazard maps, June 1996 documentation, *U.S. Geol. Surv. Open-File Rept.*, 96-532.

GELLER, R.J. (1976): Scaling relations for earthquake source parameters and magnitudes, *Bull. Seismol. Soc. Am.*, **66**, 1501-1523.

HADLEY, D.M. and D.V. HELMBERGER (1980): Simulation of strong ground motions, *Bull. Seismol. Soc. Am.*, **70**, 617-630.

HANKS, T.C. (1982): f_{max}, *Bull. Seismol. Soc. Am.*, **72**, 1867-1879.

HANKS, T.C. and R.K. MCGUIRE (1981): The character of high frequency strong ground motion, *Bull. Seismol. Soc. Am.*, **71**, 2071-2095.

HARTZELL, S. (1978): Earthquake aftershocks as Green's functions, *Geophys. Res. Lett.*, **5**, 1-4.

HASKELL, N.A. (1964): Radiation pattern of surface waves from point source in a multi-layered medium, *Bull. Seismol. Soc. Am.*, **54**, 377-393.

HATZFELD, D., V. KARAKOSTAS, M. ZIAZIA, G. SELVAGGI, S. LEBORGNE, C. BERGE, R. GUIGUET, A. PAUL, P. VOIDOMATIS, D. DIAGOURTAS, I. KASSARAS, I. KOUTSIKOS, K. MAKROPOULOS, R. AZZARA, M. DI BONA, S. BACCHESCHI, P. BERNARD and C. PAPAIOANNOU (1997): The Kozani-Grevena (Greece) earthquake of 13 May 1995 revisited from a detailed seismological study, *Bull. Seismol. Soc. Am.*, **87**, 463-473.

IRIKURA, K. (1983): Semi-empirical estimation of strong ground motions during large earthquakes, *Bull. Disas. Prev. Res. Inst., Kyoto Univ.*, **33**, 63-104.

IRIKURA, K. (1986): Prediction of strong acceleration motion using empirical Green's function, in *Proceedings 7th Japan Earthquake Engineering Symposium*, 151-156.

IRIKURA, K. and K. KAMAE (1994): Estimation of strong ground motion in broad-frequency band based on a seismic source scaling model and an empirical Green's function technique, *Ann. Geofis.*, **37** (6), 1721-1743.

KAMAE, K., P.-Y. BARD and K. IRIKURA (1998): Prediction of strong ground motion at EUROSEISTEST site using the empirical Green's function method, *J. Seismol.*, **2**, 193-207.

KANAMORI, H. (1979): A semi-empirical approach to prediction of long-period ground motions from great earthquakes, *Bull. Seismol. Soc. Am.*, **69**, 1645-1670.

KEILIS-BOROK, V. (1959): On the estimation of the displacement in an earthquake source and of source dimensions, *Ann. Geofis.*, **12**, 205-214.

MARGARIS, B.N. and D.M. BOORE (1998). Determination of $\Delta\sigma$ and κ_0 from response spectra of large earthquakes in Greece, *Bull. Seismol. Soc. Am.*, **88**, 170-182.

MARGARIS, B.N. and P. HATZIDIMITRIOU (1997): Source parameters of the Arnea earthquake, $M_s = 5.8$, based on stochastic simulation method, in *Proceedings III Hellenic Geotechnical Engeneering Congress*, March 20-22, 1997, Patras, vol. 1, 503-510 (in Greek).

MARGARIS, B.N. and B.C. PAPAZACHOS (1994): Seismic hazard simulation of strong motion based on source parameters in the area of Greece, in *Proceedings XXIV General Assembly ESC, September 19-24, 1994, Athens*, vol. 3, 1389-1397.

PAPAGEORGIOU, A.S. (1988): On two characteristic frequencies of acceleration spectra: patch corner frequency and f_{max}, *Bull. Seismol. Soc. Am.*, **78**, 509-529.

PAPAGEORGIOU, A.S. and K. AKI (1983): A specific barrier model for the quantitative description of inhomogeneous faulting and the prediction of strong ground motion. I. Description of the model, *Bull. Seismol. Soc. Am.*, **73**, 693-722.

PAPASTAMATIOU, D., V. MARGARIS and N. THEODULIDIS (1993): Estimation of the parameters controlling strong ground motion from shallow earthquakes in Greece, in *Proceedings 2nd Hellenic Geophysics Congress*, May 5-7, 1993, Florina, vol. 1, 192-201.

PAPAZACHOS, C.B. and G. NOLET (1997): *P* and *S* deep velocity structure of the Hellenic area obtained by robust non-linear inversion of travel times, *J. Geophys. Res.*, **100** (B7), 12405-12422.

PAPAZACHOS, B.C. and C. PAPAZACHOU (1997): *The Earthquakes of Greece* (Ziti Publ. Co.), pp. 356.

PAPAZACHOS, B.C., CH.A. PAPAIOANNOU, C.B. PAPAZACHOS and A.S. SAVVAIDIS (1997): *Atlas of Isoseismal Maps for Strong Shallow Earthquakes in Greece and Surrounding Area (426 B.C.-1995)* (Ziti Publ. Co.), pp. 176.

PAPAZACHOS, B.C., B.G. KARAKOSTAS, A.A. KIRATZI, E.E. PAPADIMITRIOU and C.B. PAPAZACHOS (1998): A model for the 1995 Kozani-Grevena seismic sequence, *J. Geodyn.*, **26** (2-4), 217-231.

PAVLIDES, S.B., N.C. ZOUROS, A.A. CHATZIPETROS, D.S. KOSTOPOULOS and D.M. MOUNTRAKIS (1995): The 13th May 1995 Western Macedonia, Greece, Kozani Grevena Earthquake; preliminary results, *Terra Nova*, **7**, 544-549.

THEODULIDIS, N. and P.-Y. BARD (1995): Strong ground motion simulation of large earthquakes, in *Proceedings 10th ECEE*, 269-274.

THEODULIDIS, N. and P.-Y. BARD (1998): Dependence of f_{max} on site geology: A preliminary study of Greek strong-motion data, in *Proceedings 11th ECEE, September 6-11, 1998*, vol. 1, 269-274.

TOLIS, S.B. and K. PITILAKIS (1993): SEISMOS: an algorithm for the calculation of artificial bedrock accelerograms, in *Proceedings 2nd Hellenic Geophysics Congress, May 5-7, 1993, Florina*, vol. 1, 236-247 (in Greek).

TORO, G. and R. MCGUIRE (1987): An investigation into earthquake ground motion characteristics in Eastern North America, *Bull. Seismol. Soc. Am.*, **77**, 468-489.

TSELENTIS, G.A., G. KOUKIS, E. SOKOS, D. RUBAS, J. JANSKY, V. PLICKA, M. PAKZAD and J. ZAHRADNIK (1996): Modelling the strong ground motions in the city of Patras, Greece, during July 1993 earthquake, in *Proceedings 11th World Conference Earthquake Engeneering, Acapulco, Mexico*, 381-392.

(received April 7, 2000;
accepted October 3, 2000)